Received: 15 July 2021 | Revised: 4 December 2021 | Accepted: 7 December 2021

DOI: 10.1111/cas.15241

ORIGINAL ARTICLE

Cancer Science WILEY

PolyI:C attenuates transforming growth factor-β signaling to induce cytostasis of surrounding cells by secreted factors in triple-negative breast cancer

Yusuke Tamura[1] | Shuichi Tsutsumi[2] | Kohei Miyazono[1] | Daizo Koinuma[1]

[1]Department of Molecular Pathology, Graduate School of Medicine, The University of Tokyo, Tokyo, Japan

[2]Genome Science Division, Research Center for Advanced Science and Technology, The University of Tokyo, Tokyo, Japan

Correspondence
Daizo Koinuma, Department of Molecular Pathology, Graduate School of Medicine, The University of Tokyo, 7-3-1 Bunkyo-ku, Tokyo 113-0033, Japan.
Email: koinuma@m.u-tokyo.ac.jp

Funding information
Japan Society for the Promotion of Science (JSPS) KAKENHI Grants-in-Aid for Scientific Research, Grant/Award Number: (S) (15H05774) and (A) (20H00513); JSPS Research Fellowship for Young Scientists, Grant/Award Number: DC1

Abstract

The activation of RIG-I-like receptor (RLR) signaling in cancer cells is widely recognized as a critical cancer therapy method. The expected mechanism of RLR ligand-mediated cancer therapy involves the promotion of cancer cell death and strong induction of interferon (IFN)-β that affects the tumor microenvironment. We have recently shown that activation of RLR signaling in triple-negative breast cancer cells (TNBC) attenuates transforming growth factor-β (TGF-β) signaling, which partly contributes to the promotion of cancer cell pyroptosis. However, the consequences of suppression of TGF-β signaling by RLR ligands with respect to IFN-β-mediated tumor suppression are not well characterized. This study showed that transfection of a typical RLR ligand polyI:C in cancer cells produces significant levels of IFN-β, which inhibits the growth of the surrounding cancer cells. In addition, IFN-β-induced cell cycle arrest in surrounding cancer cells was inhibited by the expression of constitutively active Smad3. Constitutively active Smad3 suppresses IFN-β expression through the alleviation of IFN regulatory factor 3 binding to the canonical target genes, as suggested by ChIP sequencing analysis. Based on these findings, a new facet of the protumorigenic function of TGF-β that suppresses IFN-β expression is suggested when RLR-mediated cancer treatment is used in TNBC.

KEYWORDS
IFN-β, IRF3, polyI:C, TGF-β, TNBC

1 | INTRODUCTION

Triple-negative breast cancer is an aggressive cancer, and patients develop resistance to anticancer drugs, leading to poor prognosis.[1,2] One of the novel methods suggested for TNBC treatment is the activation of RLR signaling in cancer cells by transfection of RLR ligands, such as polyI:C, to induce tumor cell death.[3-5]

One of the possible difficulties of transfection-based approaches for cancer therapy is the limited efficiency of intracellular delivery of nucleic acids; the ligands might not be necessarily delivered to all cancer cells.[6] However, cytosolic administration of RLR ligands is also expected to overcome this issue by affecting surrounding, untransfected cells through enhanced production of IFNs.[3,4] Interferons are a group of ligands released when cells are invaded by pathogens

Abbreviations: caSmad, constitutively active Smad3; ChIP-seq, ChIP sequencing; gRNA, guide RNA; IFN, interferon; IFNAR, interferon alpha and beta receptor; IRF, interferon regulatory factor; ISG, interferon-stimulated gene; PRD, positively regulated domain; qPCR, quantitative PCR; RIG-I, retinoic acid-inducible gene-I; RLR, RIG-I-like receptor; STAT, signal transducer and activator of transcription; TGF-β, transforming growth factor β; TNBC, triple-negative breast cancer.

to activate innate and adaptive immune responses. Interferon-β is considered as one of the most important IFNs because IFN-β binds strongly to the receptors IFNAR1 and IFNAR2.[7,8] After receptor binding, Jak2 and Tyk1 interact with the receptors, which is followed by phosphorylation of STAT1 and STAT2. Phosphorylated STAT1 and STAT2 then form a complex with IRF9 and upregulate a group of genes called ISGs to confront pathogens. However, the effect of IFN-β secreted by cancer cells through the administration of virus-mimicking RLR ligands in the context of cancer treatment has not been examined in detail.

Transforming growth factor-β is one of the main contributors to tumor progression in TNBC. Our previous report showed that the transfection of polyI:C, which is a classically used RLR ligand and is being currently evaluated in clinical trials for cancer treatment, suppresses TGF-β signaling and accelerates tumor cell death.[9] Our interests, therefore, expand to the question of whether polyI:C-induced suppression of TGF-β signaling also influences IFN-β expression and attenuates the functional effect of IFN-β on surrounding cancer cells.

2 | MATERIALS AND METHODS

2.1 | Cell culture

BT-549 and Hs578T cells were from ATCC and cultured in RPMI-1640 medium (#11875; Thermo Fisher Scientific) supplemented with 10% FBS (#SH30910.03 #10270-106; Thermo Fisher Scientific), 50 U/mL penicillin, 50 μg/mL streptomycin, and 0.95 μg/mL (BT-549) or 10 μg/mL (Hs578T) insulin. The cells were maintained in a 5% CO_2 atmosphere at 37°C.

2.2 | Statistical analysis

Welch's *t* test was used to compare the two samples, and Tukey-Kramer (for comparison of all combinations) or Dunnett tests (for comparison with a control) were used to compare multiple samples.

Additional materials and methods are available in Appendix S1. Primer sequences are available in Table S1.

3 | RESULTS

3.1 | PolyI:C transfection produces sufficient levels of IFN-β that cause inhibition of cell growth in TNBC

We first evaluated whether the IFN-β ligand activates the IFN pathway in BT-549, a TNBC cell line. We found that the ng/mL-order of IFN-β is sufficient to phosphorylate STAT1, which is a downstream phosphorylation target of the IFN-β receptors in BT-549 cells (Figure 1A). We next analyzed the biological effect of IFN-β and found that 3 or 4 days of stimulation with IFN-β suppressed the proliferation of BT-549 cells (Figure 1B). This might be partially mediated by the induction of *CDKN1A*, as previously reported (Figure 1C).[10,11] We next examined whether transfection of polyI:C induces the secretion of IFN-β from BT-549 cells at a functional level. Less than 10 pg/mL IFN-β was secreted by mock transfection conditions, whereas approximately 1 ng/mL IFN-β was secreted after 6 hours of polyI:C transfection, and more than 3 ng/mL was secreted after 24 hours, both of which were sufficient to activate the IFN-β pathway and phosphorylate STAT1 (Figure 1D). These results suggest that polyI:C transfection produces sufficient levels of IFN-β, which can possibly lead to growth inhibition of surrounding cancer cells.

3.2 | PolyI:C-induced suppression of TGF-β signaling further escalates IFN-β production

We previously reported that polyI:C transfection in TNBC inhibited TGF-β signaling through attenuation of Smad3 phosphorylation, and this suppression promoted tumor cell death.[9] The next question is whether polyI:C-induced attenuation of TGF-β signaling also accelerates IFN-β production, which is also one of the major expected benefits of RLR ligands for cancer therapy. To inhibit the exhaustion of TGF-β signaling by polyI:C transfection, we used BT-549 cells stably expressing caSmad3 (BT-549-caSmad3 cells) with upregulated expression of a target gene of TGF-β, *PMEPA1* (Figure S1A). We used BT-549 cells stably expressing HA (BT-549-HA cells) as a control. PolyI:C transfection in BT-549-caSmad3 cells significantly suppressed the mRNA expression of *IFNB1* (Figure 2A) and the early phase of IFN-β production (Figure 2B), although the decrease in IFN-β production by caSmad3 was minimal after 24 hours of polyI:C transfection. In agreement with the result of caSmad3 expression, pretreatment of the cells with TGF-β, instead of caSmad3 expression, also partially attenuated the induction of *IFNB1* (Figure S1B). To test whether coculturing polyI:C-transfected cells with intact cells alleviated the proliferation of intact cells, we used a coculture system and evaluated the cell growth of intact cells by staining with crystal violet (Figure 2C, upper panels). By coculture with polyI:C-transfected BT-549-HA cells, the growth of parental BT-549 cells was significantly attenuated, suggesting that factors including IFN-β secreted from BT-549-HA cells triggered growth inhibition of the surrounding, untransfected cells. In contrast, the inhibitory effect was not significant when polyI:C was transfected into BT-549-caSmad3 cells (Figure 2C, lower panels, and 2D).

Interferon regulatory factor 3 is one of the critical transcription factors that contribute to the induction of IFN-β during the early response to viral infection.[12] Thus, we evaluated the transcriptional activity of IRF3 using a luciferase reporter vector, PRDIII-I, which contains IRF3 binding sites upstream of the *IFNB1* gene locus.[13] The caSmad3 expression in BT-549 cells significantly attenuated the activity of 3× (PRDIII-I)-Luc, suggesting that the function of IRF3 is impaired by caSmad3 in BT-549-caSmad3 cells (Figure 2E). This

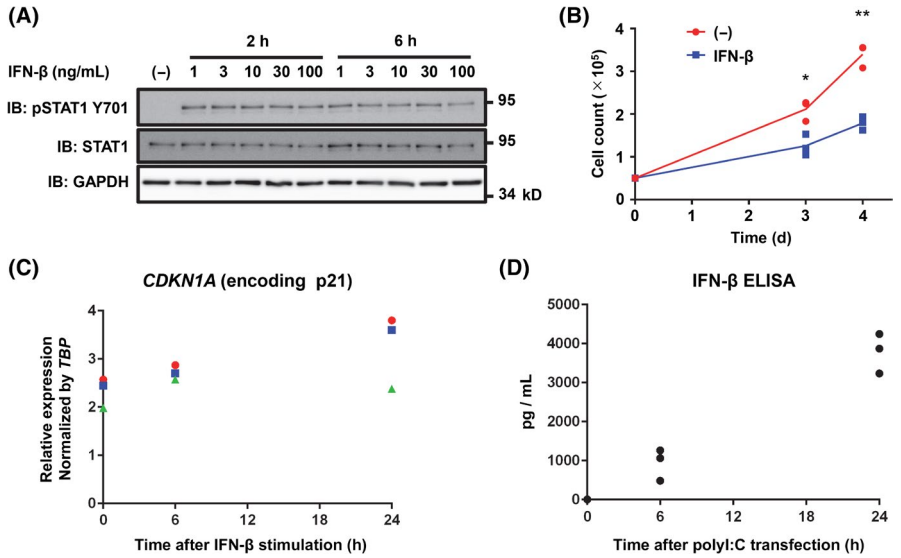

FIGURE 1 PolyI:C transfection produces functional levels of interferon-β (IFN-β) to induce cytostatic effect. A, Immunoblotting analysis of phosphorylated signal transducer and activator of transcription 1 (STAT1) after stimulation with IFN-β in triple-negative breast cancer cells. Phosphorylation of STAT1 by IFN-β was detected by the phosphorylation of tyrosine-701 (Y701). BT-549 cells were stimulated with the indicated concentrations of IFN-β for 2 or 6 h, and the lysed cells were analyzed by immunoblotting (IB). A representative of two independent experiments is shown. B, Effect of IFN-β on cell growth in BT-549 cells. BT-549 cells were stimulated with IFN-β (10 ng/mL) on day 0, and the cells were collected and enumerated by Trypan blue staining after 3 or 4 d of culture. Data were obtained from three independent experiments. $^{*}P < .05$, $^{**}P < .01$, Welch's *t* test. C, Quantitative RT-PCR analysis of *CDKN1A* (encoding p21 protein) in IFN-β-stimulated BT-549 cells. BT-549 cells were stimulated with IFN-β (10 ng/mL) for 6 or 24 h, or left untreated. Data were normalized to *TBP* expression. Data were obtained from three independent experiments (shown in red, blue, and green). D, ELISA of secreted IFN-β after transfection of polyI:C. BT-549 cells were transfected with polyI:C (1 μg/mL), and the culture supernatant was collected after 6 or 24 h of transfection. Data were obtained from three independent experiments

is supported by the finding that upregulation of *ISG15* by polyI:C, which is also a target of IRF3,[14] was alleviated in BT-549-caSmad3 cells (Figure S1C), and also partially attenuated by TGF-β pretreatment in parental BT-549 cells (Figure S1D).

We then confirmed our findings by using another TNBC cell line, Hs578T. Hs578T cells were also prone to polyI:C-induced cell death, partly through the inhibition of TGF-β signaling, in our previous study.[9] Hs578T cells stably expressing either caSmad3 (Hs578T-caSmad3) or HA (Hs578T-HA) were established, and we found that caSmad3 expression in Hs578T cells inhibited *IFNB1* induction by polyI:C (Figure 2F). We also used another experimental setting to evaluate the effect of polyI:C-induced secreted factor(s) on the cell proliferation of untransfected cells by collecting conditioned media from Hs578T-caSmad3 and Hs578T-HA cells. Similar to the result of the coculture of BT-549-caSmad3 cells, conditioned media from Hs578T-caSmad3 cells partly inhibited the cytostatic effect of polyI:C (Figure 2G). Xu et al[15] previously revealed the polyI:C-induced suppression of Smad signaling in several types of cells. To know whether the expression of *IFNB1* by polyI:C is also affected by TGF-β in other types of cancer, we evaluated HepG2 based on their findings. Unlike BT-549 and Hs578T cells, *IFNB1* expression in HepG2 cells was not inhibited, but rather induced by TGF-β (Figure S1E), suggesting cell type-specific regulatory mechanisms.

These results indicate that suppression of TGF-β signaling by polyI:C promotes IFN-β secretion, which results from the enhanced IRF3 function through suppression of TGF-β signaling in BT-549 and Hs578T cells.

We next examined the effect of neutralizing Abs against IFN-β on cell proliferation. Coculturing of nontransfected cells with polyI:C-transfected cells revealed that neutralizing Abs against IFN-β did not rescue the nontransfected cells from growth inhibition by coculture with polyI:C-transfected cells (Figure S2A–C), suggesting that IFN-β is not the only factors downstream of polyI:C to suppress cell proliferation of surrounding untransfected cells. Therefore, we evaluated the expression of other secreted factors possibly induced by polyI:C. To this end, we picked up *IFNA1*, *IFNA2*, *IFNA8*, and *IFNA17*, as type I IFNs related to breast cancer.[16-19] We also evaluated the expression of other type I IFNs, *IFNE* and *IFNW1*, as potential targets of IRF3 downstream of polyI:C. The result showed, however, very weak expression of these factors and the absence of induction by polyI:C, in contrast to *IFNB1* and a type III IFN, *IFNL1* (see below; Figure S2D). Because there are more than 15 known type I IFNs, we then knocked down their common receptor, IFNAR1, to inhibit the signaling pathway[20] (Figure S2E). BT-549 cells transfected with IFNAR1 siRNAs were cultured with conditioned media obtained from parental BT-549 cells transfected with or without polyI:C. Unfortunately, consistent results were not obtained between the two siRNAs targeting IFNAR1 regarding the cytostatic effect of polyI:C (Figure S2F). Indeed, we found that *IFNL1* (encoding IFN-λ1 protein), a member of the type III IFN family that is not generally considered to bind to *IFNAR1* and likely caused the phosphorylation of STAT1, was also

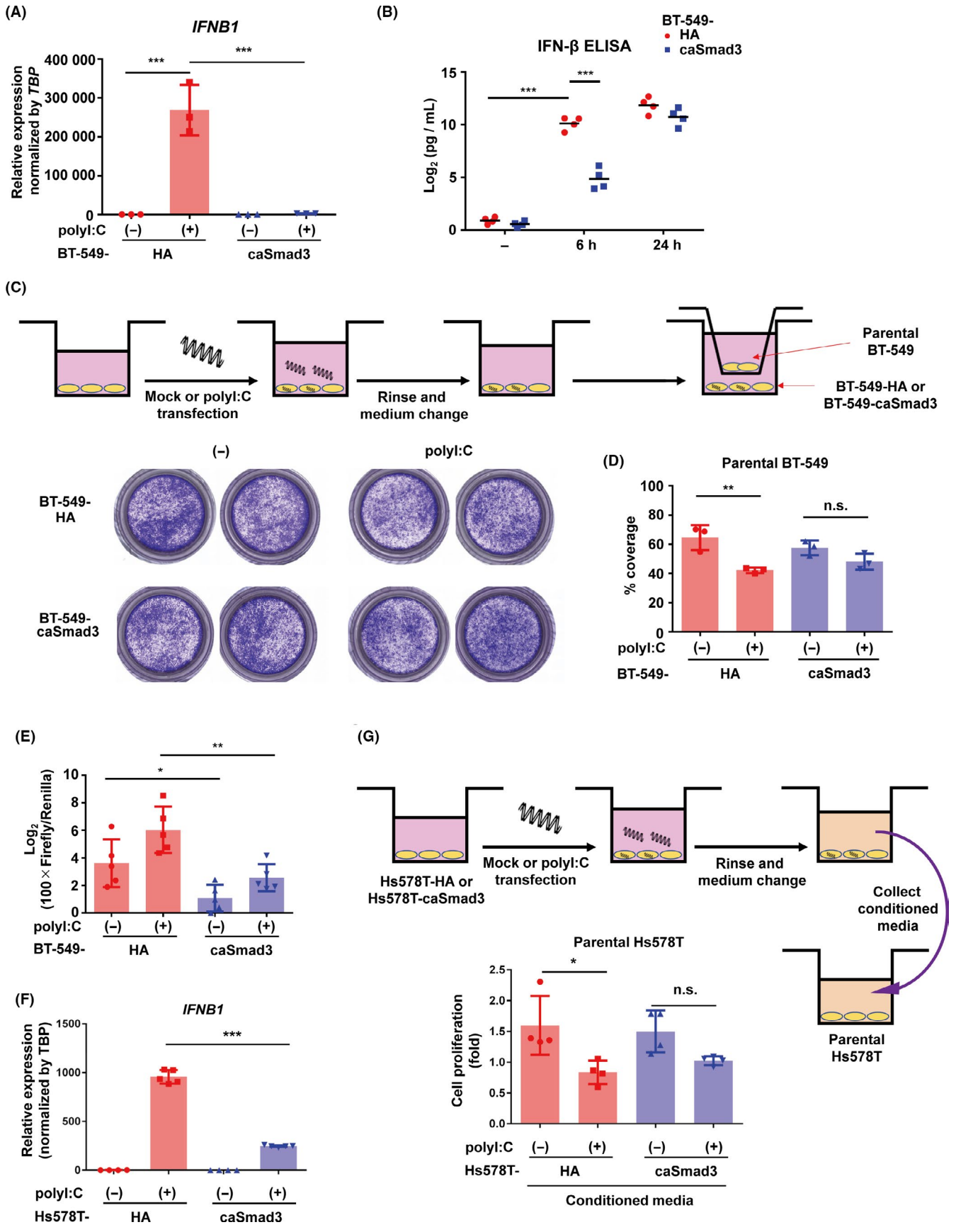
(A)
IFNB1
Relative expression normalized by TBP
400 000
300 000
200 000
100 000
0
***
***
polyI:C (–) (+) (–) (+)
BT-549- HA caSmad3
(B)
IFN-β ELISA
BT-549-
HA
caSmad3
Log2 (pg / mL)
15
10
5
0
***
***
–
6 h
24 h
(C)
Mock or polyI:C transfection
Rinse and medium change
Parental BT-549
BT-549-HA or BT-549-caSmad3
(–)
polyI:C
BT-549- HA
BT-549- caSmad3
(D)
Parental BT-549
% coverage
100
80
60
40
20
0
**
n.s.
polyI:C (–) (+) (–) (+)
BT-549- HA caSmad3
(E)
Log2 (100 × Firefly/Renilla)
10
8
6
4
2
0
**
*
polyI:C (–) (+) (–) (+)
BT-549- HA caSmad3
(F)
IFNB1
Relative expression (normalized by TBP)
1500
1000
500
0
***
polyI:C (–) (+) (–) (+)
Hs578T- HA caSmad3
(G)
Hs578T-HA or Hs578T-caSmad3
Mock or polyI:C transfection
Rinse and medium change
Collect conditioned media
Parental Hs578T
Parental Hs578T
Cell proliferation (fold)
2.5
2.0
1.5
1.0
0.5
0.0
*
n.s.
polyI:C (–) (+) (–) (+)
Hs578T- HA caSmad3
Conditioned media

FIGURE 2 Constitutively active Smad3 (caSmad3) suppresses interferon-β (IFN-β) expression induced by polyI:C transfection. A, Quantitative RT-PCR analysis of *IFNB1* (encoding IFN-β) in BT-549-HA and BT-549-caSmad3 cells transfected with polyI:C. Cells were transfected with polyI:C (1 μg/mL), and total RNA was collected after 6 h of transfection. Data were obtained from three independent experiments. B, ELISA of the secreted IFN-β after transfection of polyI:C. BT-549-HA or BT-549-caSmad3 cells were transfected with polyI:C (1 μg/mL) and the culture supernatant was collected after 6 or 24 h of transfection. Data were obtained from four independent experiments. C, D, Effect of caSmad3-induced suppression of IFN-β on the growth of cocultured BT-549 cells. BT-549-HA or BT-549-caSmad3 cells were transfected with polyI:C (1 μg/mL). The culture medium was changed to remove polyI:C 6 h after transfection, and parental BT-549 cells were seeded on the cell culture insert (C, top panels). After 4 d of coculture, parental cells were fixed and stained with crystal violet. Representative images of cocultured cells under each condition (C, bottom panels). Percent coverage of cocultured cells on the cell culture insert (D). Data were obtained from three independent experiments. E, Interferon regulatory factor 3-responsive luciferase assay after transfection of polyI:C in BT-549-HA or BT-549-caSmad3 cells. 3× (PRDIII-I)-Luc derived from the *IFNB1* promoter and CMV-Renilla vectors were transfected into BT-549-HA or BT-549-caSmad3 cells. After 18 h of reporter transfection, cells were transfected with polyI:C and incubated for 6 h. Data were obtained from five independent experiments. F, Expression of *IFNB1* in Hs578T cells stably expressing caSmad3 (Hs578T-caSmad3) or HA (Hs578T-HA). Total RNA was collected 6 h after transfection with polyI:C as in (A). Data were obtained from four (HA) or five (caSmad3) biological replicates. G, Effect of caSmad3 expression on the secreted factors from Hs578T cells related to cellular proliferation. Parental Hs578T cells were cultured with the conditioned media obtained from the Hs578T-caSmad3 or Hs578T-HA cells transfected with or without polyI:C for 3 d, and cell numbers were counted. Data were obtained from four biological replicates. Error bars, SD. $^{*}P < .05$, $^{**}P < .01$, $^{***}P < .001$, Tukey-Kramer test. n.s., not significant

strongly induced by polyI:C transfection and suppressed by caSmad3 (Figure S2D,G). Based on the findings that IFN-β protein is expressed at a sufficient level to inhibit cell proliferation (Figure 1A,B,D), IFN-β is at least the representative type I IFN induced by polyI:C in BT-549 cells, and other secreted factors such as IFN-λ1 contribute to the tumor-suppressive potential of polyI:C transfection.

3.3 | Chromatin immunoprecipitation sequencing analysis elucidates the genome-wide IRF3 regulation in BT-549-caSmad3 cells

The above results suggested that the function of IRF3 was attenuated in caSmad3-expressing BT-549 cells. However, we previously failed to find a significant difference in phosphorylation of IRF3 Ser386 between BT-549-HA cells and BT-549-caSmad3 cells after 18 hours of polyI:C transfection.[9] Therefore, we undertook ChIP analyses of IRF3 and Smad3 binding to DNA in BT549-HA or BT-549-caSmad3 cells. We first undertook ChIP-qPCR, and found that the most remarkable binding of IRF3 to the regulatory region of *IFNB1* and *ISG15* was observed after 2-4 hours of polyI:C transfection (Figure 3A).

Chromatin immunoprecipitation sequencing was then carried out by an established method[21,22] to determine the genome-wide distribution of IRF3 and Smad3 in BT-549-HA and BT-549-caSmad3 cells (Figure 3B). The effect of polyI:C on Smad3 binding was evaluated by comparing ChIP-seq data of BT-549-HA cells with or without polyI:C transfection (Figure S3A). The number of Smad3 binding regions was increased in caSmad3-expressing cells, suggesting a relatively weak strength of the Smad3 signaling pathway in the BT-549-HA cells (Figure S3B). De novo motif analysis of the IRF3 binding regions in BT-549-HA cells showed that the IRF binding site was the most significant motif, suggesting the validity of the data (Figure 3C).

The number of IRF3 binding regions was increased in BT-549-caSmad3 cells (Figure 3D). However, a comparison of the IRF3 and Smad3 binding regions in BT-549-HA and BT-549-Smad3 showed that only 1266 and 1841 IRF3 binding regions were shared with Smad3, respectively (Figure 3E). We found that IRF3 binding at known target gene loci, such as *ISG15*, *IFIT1*, and *IFNB1*, was strongly downregulated in BT-549-caSmad3 cells (Figure 3F). Notably, significant Smad3 binding was not observed at these loci. In contrast, the IRF3 binding strength was not inhibited at the *ID1* locus, a known target of Smad3 (Figure S3C, left). As a negative control, we did not identify significant IRF3 or Smad3 binding regions at the *HBB* locus (Figure S3C, right).

We further analyzed the ChIP-seq data to determine the characteristics of IRF3 binding regions specific to either BT-549-HA or BT-549-caSmad3 cells. In the BT-549-HA cell-specific IRF3 binding regions, motif analysis again showed significant IRF3 binding motif enrichment (Figure 4A). The IRF3 binding motifs were enriched in the peak summit of the binding regions (Figure 4B), whereas motifs identified in the IRF3 binding regions found in both cells (BT-549-HA and BT-549-caSmad3) or those specific to BT-549-caSmad3 cells did not show notable features (Figure S4A,B). Nor did we find an IRF3 binding motif in the Smad3 binding regions in BT-549-caSmad3 cells (Figure S4C). Gene ontology analysis of IRF3 binding regions specific to BT-549-HA cells showed enrichment of IFN signaling-related ontologies (Figures 4C,D and S5A,B). Many of the well-known targets of IRF3 were included in this group (Figure 3F). Interestingly, the IRF3-bound genes common to both BT-549-HA and BT-549-caSmad3 cells and those specific to BT-549-caSmad3 cells are not widely accepted as canonical targets of IFN signaling (Figure S5C–F). The IRF3 and Smad3 binding signals flanking the peak summits of all IRF3 binding regions (union of the IRF3 binding regions in both BT-549-HA and BT-549-caSmad3 cells) were then visualized (Figure 4E). The IRF3 binding signals were downregulated in BT-549-caSmad3 cells compared to BT-549-HA cells in the IRF3 binding regions specific to BT-549-HA cells at the genome-wide level, which was in agreement with the data at *IFNB1*, *ISG15*, and *IFIT1* loci (Figure 3F). In contrast, this inhibitory effect of caSmad3 expression was not observed in IRF3 binding regions specific to BT-549-caSmad3 cells or in the binding regions common to BT-549-HA and BT-549-caSmad3 cells. The frequency of Smad3-cobinding was 9.7% in the

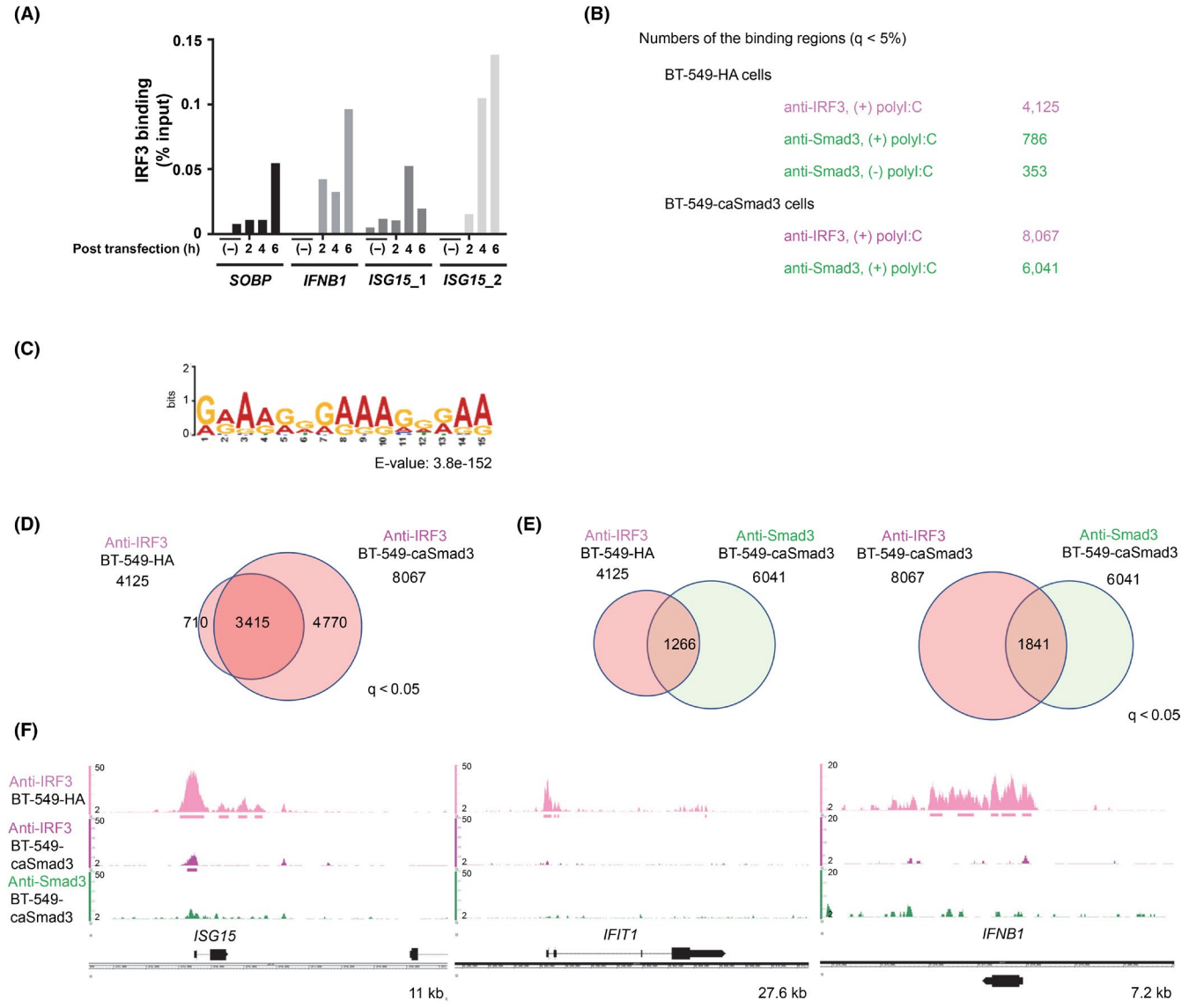

FIGURE 3 Chromatin immunoprecipitation sequencing (ChIP-seq) analysis of interferon regulatory factor 3 (IRF3) and Smad3 in BT-549-HA and BT-549-constitutively active Smad3 (caSmad3) cells. A, ChIP-quantitative PCR analysis of IRF3 in polyI:C-transfected BT-549 cells. Cells were fixed after 2, 4, and 6 h of transfection. Percent input of immunoprecipitated DNA around indicated gene loci is shown. Binding of IRF3 to the *SOBP* locus served as a control. B, ChIP-seq analysis identified IRF3 and Smad3-binding regions in BT-549-HA and BT-549-caSmad3 cells. After 4 h of transfection with polyI:C, the cells were fixed and harvested, and anti-IRF3 ChIP-seq analyses were carried out in BT-549-HA and BT-549-caSmad3 cells. To compare the IRF3 ChIP-seq data with Smad3 ChIP-seq data in BT-549-caSmad3 cells, anti-Smad3 ChIP-seq data were obtained from transforming growth factor-β-treated (1.5 h) BT-549-HA cells with (+) or without (–) polyI:C transfection. Significant binding regions were calculated from the pool of ChIP-seq data obtained from the two biological replicates. The number of binding regions identified is shown. C, De novo motif prediction identified the IRF binding motif in the IRF3 ChIP-seq data of BT-549-HA cells. The most significant motif is shown with the E-value. D, A Venn diagram showing the overlap of the IRF3 binding regions between BT-549-HA and BT-549-caSmad3 cells. The number of cell-specific IRF3 binding regions in BT-549-HA and BT-549-caSmad3 cells was 710 and 4770, respectively. E, Limited overlaps between IRF3 and Smad3 binding regions in BT-549-HA and BT-549-caSmad3 cells. F, Reduced IRF3 binding in the *ISG15*, *IFIT1*, and *IFNB1* loci in BT-549-caSmad3 cells (middle panel) relative to BT-549-HA cells (top panel). Significant Smad3 binding was absent in those regions (bottom panel). Y-axis shows the values calculated by MACS2 (arbitrary units)

IRF3 binding regions specific to BT-549-HA cells, whereas it was as high as 35.1% in the common IRF3 binding regions. We validated the downregulation of IRF3 binding in BT-549-caSmad3 cells through ChIP-qPCR (Figure 4F).

We then established BT-549 cells with Smad3 gene inactivation to evaluate the contribution of the endogenous signaling pathway to inhibit polyI:C-induced *IFNB1* expression and cytostasis. Of note, Smad3 was phosphorylated at baseline in both BT-549 and Hs578T cells,[9] but too weak to detect, depending on the experimental condition (Figure 5A). Stable Smad3 gene inactivation was achieved by lentivirus-based gRNA expression (Figure 5A). We found an enhancement of polyI:C-induced transcriptional activity of the 3×

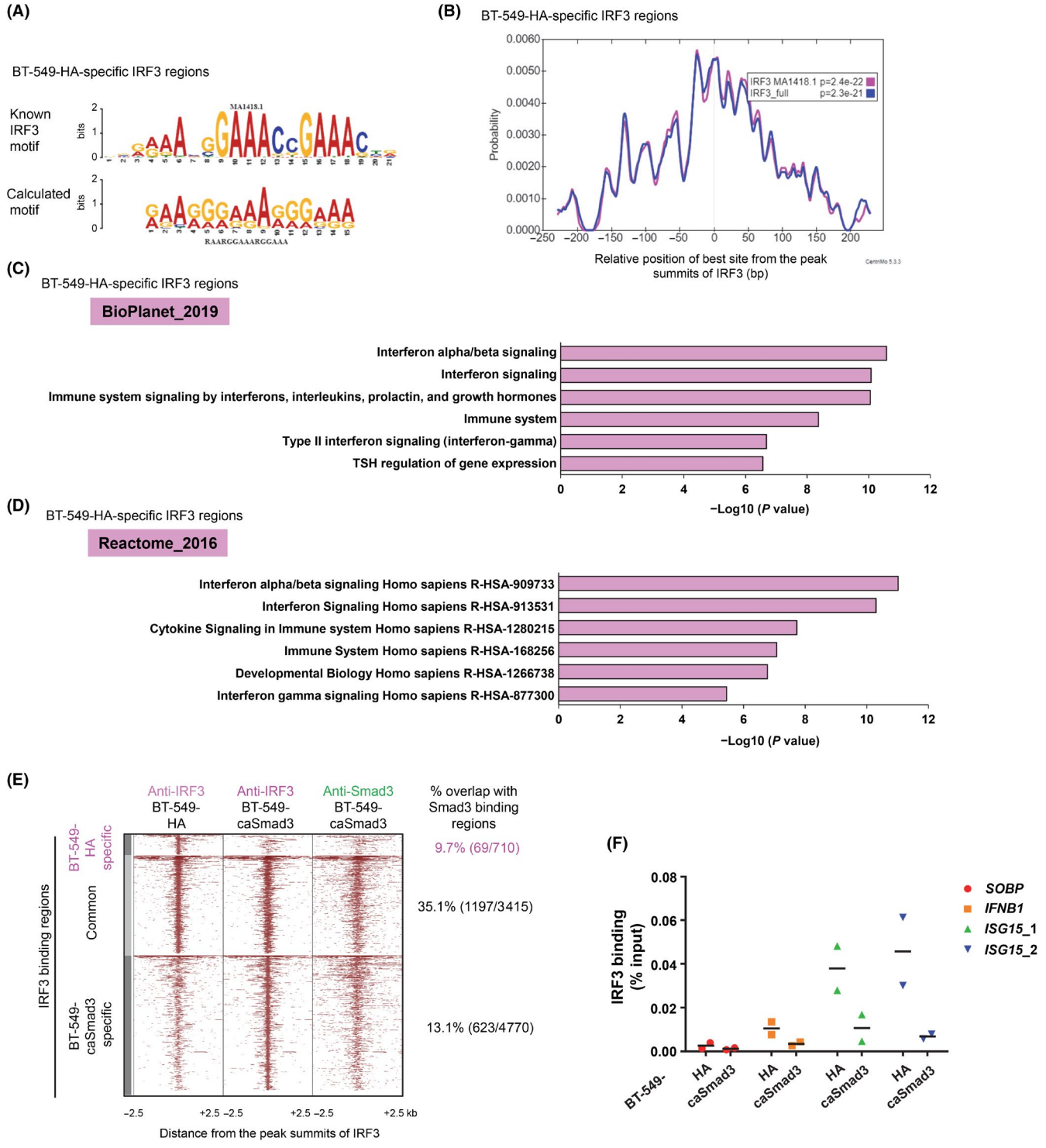

FIGURE 4 Expression of genes related to interferon signaling regulated by interferon regulatory factor 3 (IRF3) is suppressed in BT-549-constitutively active Smad3 (caSmad3) cells. A, Results of de novo motif prediction of IRF3 binding regions specific to BT-549-HA cells. The known IRF3 binding motif (upper panel) and the most significant motif (bottom panel) of the IRF3 binding regions specific to BT-549-HA cells are shown. B, Centrality analysis of the motif identified in (A). Position of the best site relative to the peak summit of each IRF3 binding region is shown. The identified IRF3 motifs were present in 34% (239/710) of the IRF3 binding regions specific to BT-549-HA cells. C, D, Gene ontology analysis of IRF3-bound genes specific to BT-549-HA cells. 898 genes were analyzed using gene ontology datasets "BioPlanet_2019" (C) and "Reactome_2016" (D). The top six enriched ontologies ($P < .05$) are shown. E, Comparison of IRF3 binding regions between BT-549-HA and BT-549-caSmad3 cells. IRF3 binding regions (union of IRF3 binding regions of BT-549-HA and BT-549-caSmad3 cells) were classified into three groups based on the results shown in Figure 3D. IRF3 and Smad3 binding signals of ChIP sequencing data relative to the peak summits of IRF3 binding regions were visualized to show their binding strength and proximity. The percentage of the presence of significant Smad3 binding regions in each group is also shown. F, ChIP-quantitative PCR analysis of IRF3 in polyI:C-transfected BT-549-HA or BT-549-caSmad3 cells. The percent input of immunoprecipitated DNA around the indicated gene locus is shown. The graph shows the results of two independent experiments. ChIP samples obtained prior to library preparation for ChIP sequencing were used

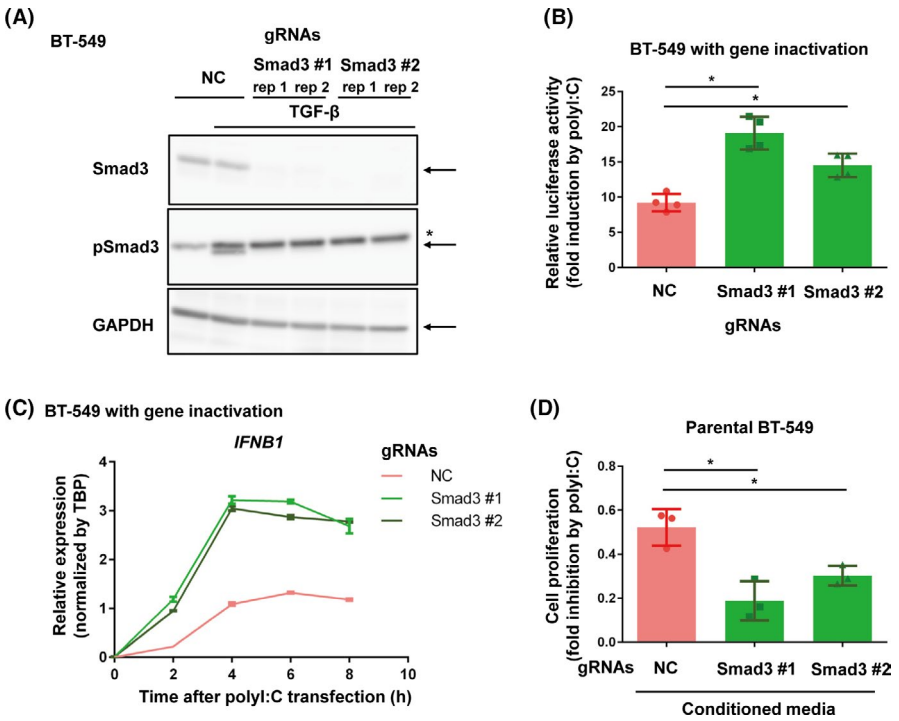

FIGURE 5 Effect of Smad3 gene inactivation on *IFNB1* expression and cellular response to polyI:C transfection. A, Immunoblotting for evaluation of Smad3 gene inactivation. BT-549 cells infected with lentiviruses expressing Smad3 or control (NC) guide RNAs (gRNAs) were stimulated with 1 μg/mL transforming growth factor-β (TGF-β) for 4 h. Smad3 gRNA-infected samples were prepared as biological duplicates (lanes 3 and 4 for Smad3 gRNA #1; lanes 5 and 6 for gRNA #2). Two blotted membranes were prepared to detect different antigens. *Nonspecific band. B, Interferon regulatory factor 3 (IRF3)-responsive luciferase assay using 3× (PRDIII-I)-Luc in polyI:C-transfected BT-549 cells with Smad3 gene inactivation. After 24 h of the reporter transfection, cells were transfected with 1 μg/mL polyI:C and incubated for 6 h. Data were obtained from four biological replicates and normalized to the relative luciferase activities (firefly/Renilla) without polyI:C transfection. C, Quantitative RT-PCR of *IFNB1* in Smad3 gene-inactivated BT-549 cells. Cells infected with gRNAs were transfected with 1 μg/mL polyI:C and incubated for the indicated times. Data were obtained as biological duplicates. D, Proliferation of BT-549 cells cultured with conditioned media prepared from gRNA-expressing cells. BT-549 cells were seeded on a 24-well plate (1×10^4 cells/well). Medium was replaced with the conditioned media on the next day and incubated for 4 d. Data were obtained from the three biological replicates and normalized to the cell numbers of respective gRNA-expressing cells without polyI:C transfection. Error bars, SD. *$P < .05$, Dunnett's test

(PRDIII-I)-Luc reporter (Figure 5B) and *IFNB1* expression (Figure 5C) by Smad3 gene inactivation. By collecting the conditioned media from the culture of Smad3 gRNA-expressing cells after polyI:C transfection, the cytostatic effect of polyI:C was also enhanced (Figure 5D). To determine whether the Smad3 gene inactivation enhances genome-wide IRF3 binding, we additionally acquired ChIP-seq data of control or Smad3 gRNA expressing cells. However, the results suggested that loss of Smad3 expression only minimally changed the distribution of IRF3 binding regions on the genome (Figure S6A). Even when focusing on the BT-549-HA-specific IRF3 binding regions identified in Figures 3F and 4E, the effect of Smad3 gene inactivation was not observed by the attempt to quantify the ChIP-seq data (Figure S6B,C). The ChIP-qPCR analysis of IRF3 binding regions also suggested the absence of statistically significant up-regulation by Smad3 gRNAs (Figure S6D). Therefore, we concluded that the residual endogenous Smad signaling after the suppression by polyI:C transfection is not enough to show detectable levels of changes in the IRF3 binding strength by ChIP experiments.

The above results suggested that the canonical target genes of the IFN signaling regulated by IRF3 were inhibited by Smad signaling in TNBC cells, which was efficiently suppressed by polyI:C in the present in vitro culture condition. Because TGF-β signaling is activated in some of the TNBC tumors in vivo,[9,23,24] the present findings suggest the importance of considering the activation of this signaling pathway for the selection of patients to treat with polyI:C.

4 | DISCUSSION

In the present study, we showed that polyI:C-transfected BT-549 cells released functional levels of IFN-β, which suppressed the growth of even nontransfected cells. It was also suggested that polyI:C-induced suppression of TGF-β signaling further promoted IFN-β secretion and growth inhibition. The mechanism of caSmad3-mediated reduction of IFN-β levels is associated with the alleviation of IRF3 function, possibly through the inhibition of IRF3 binding to the canonical target gene loci (Figure 6). The present findings revealed a mechanism of action of polyI:C in cancer cells, in addition to its propyroptotic function.[9] Importantly, the cytostatic effect

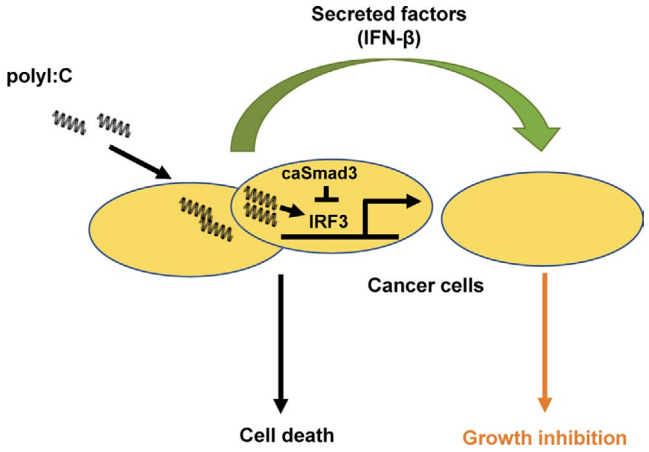

FIGURE 6 Model of the mechanism of action of therapeutic polyI:C transfection to cancer cells. Transfection of polyI:C induces pyroptotic cancer cell death as reported previously,[9] but not all the cells receive polyI:C, because of the nature of the transfection-based delivery. However, transfected polyI:C activates interferon regulatory factor 3 (IRF3) to induce interferon-β (IFN-β) and other secreted factors to inhibit the proliferation of surrounding, untransfected cancer cells. The mechanism partly involves the inhibition of transforming growth factor-β-Smad3, which suppresses IRF3 binding to its canonical target genes

through IFN-β can address the limited intracellular delivery rate of polyI:C, a common problem related to the nature of the transfection-based method. In the case of in vivo tumor, cancer cell heterogeneity could also potentially contribute to the reduced intracellular drug delivery rate by transfection.

Interferon has long attracted attention as an antitumor drug, such as for renal cancer treatment.[11,25] We showed that polyI:C-induced IFN-β suppressed the proliferation of surrounding cancer cells. However, the present observation using the neutralizing Abs against IFN-β suggested the importance of other simultaneously secreted factors (Figure S2A–C). Strong induction of *IFNL1* (encoding IFN-λ1 protein), a member of the type III IFN family, by polyI:C transfection is a possible factor for this process (Figure S2G).

In addition, lower-dose treatment with IFN-β (100 U, approximately 0.1 ng/mL) in TNBC has been reported to inhibit cancer stem cell traits or mesenchymal phenotype.[26,27] Therefore, the effect of polyI:C-induced IFN-β on these properties should also be examined in the future.

Many previous reports have revealed that TGF-β signaling and IFN signaling cross-talk with each other in immune systems. For example, while IFN activates the host immune system to prevent damage from viral infection, TGF-β suppresses the overactivation of the immune reaction or is associated with the convergence of the immune response.[28] Interferon and TGF-β signaling mutually interfere with various strata. Interferon-γ induces Smad7 to inhibit TGF-β signaling.[29] In contrast, TGF-β suppresses the production of IFN-γ in $CD4^+$ T cells by reducing the expression of TBET and STAT4 to dampen the immune reaction.[30,31] More importantly, activation of IRF3 by the RLR ligand suppresses the phosphorylation of Smad3 to attenuate regulatory T cell differentiation[15] or cancer cell pyroptosis,[9] which is based on the conformity of domains close to the C-termini of IRF3 and Smad3 necessary for molecular interaction.[32,33]

This study suggests the suppression of IRF3 function by TGF-β signaling. Although the transcriptional activity of IRF3 is reduced in caSmad3-expressing BT-549 cells, as shown by luciferase assay or ChIP-seq analysis, it is notable that it might not be the regulation of phosphorylation of the Ser386 residue of IRF3 that is crucial for IRF3 activation.[34] In addition, it is not probable that Smad3 directly binds to DNA and suppresses IRF3 function because not many peaks of IRF3 ChIP-seq specific to BT-549-HA cells were occupied by Smad3 (Figure 4E). It is possible that activated Smad3 directly or indirectly alleviates the function of IRF3, such as through posttranslational levels or regulation of nuclear translocation. Smad3 might also be redirecting the distribution of IRF3 from canonical targets to other targets, where Smad3 and IRF3 colocalize and regulate the expression of other target genes. Although further studies will be needed, uncovering these mechanisms could explain the antiimmunological function of TGF-β and highlight the therapeutic targets of various diseases, including cancer.

ACKNOWLEDGMENTS

We thank Keiko Yuki for technical assistance. This work was supported by KAKENHI Grants-in-Aid for Scientific Research (S) (15H05774) and (A) (20H00513) (KM) from the Japan Society for the Promotion of Science (JSPS). YT was supported by a JSPS Research Fellowship for Young Scientists (DC1).

DISCLOSURE

The authors have no conflicts of interest to declare.

DATA AVAILABILITY STATEMENT

Raw sequence data are available in the GEO (GSE178830 and GSE188457).

ORCID

Kohei Miyazono https://orcid.org/0000-0001-7341-0172
Daizo Koinuma https://orcid.org/0000-0001-5611-2122

REFERENCES

1. Harbeck N, Penault-Llorca F, Cortes J, et al. Breast cancer. *Nat Rev Dis Primers*. 2019;5:66.
2. Foulkes WD, Smith IE, Reis-Filho JS. Triple-negative breast cancer. *N Engl J Med*. 2010;363:1938-1948.
3. Demaria O, Cornen S, Daeron M, Morel Y, Medzhitov R, Vivier E. Harnessing innate immunity in cancer therapy. *Nature*. 2019;574:45-56.
4. Elion DL, Cook RS. Harnessing RIG-I and intrinsic immunity in the tumor microenvironment for therapeutic cancer treatment. *Oncotarget*. 2018;9:29007-29017.
5. Elion DL, Jacobson ME, Hicks DJ, et al. Therapeutically active RIG-I agonist induces immunogenic tumor cell killing in breast cancers. *Cancer Res*. 2018;78:6183-6195.
6. Durymanov M, Reineke J. Non-viral delivery of nucleic acids: insight into mechanisms of overcoming intracellular barriers. *Front Pharmacol*. 2018;9:971.

7. Mesev EV, LeDesma RA, Ploss A. Decoding type I and III interferon signalling during viral infection. *Nat Microbiol*. 2019;4:914-924.
8. McNab F, Mayer-Barber K, Sher A, Wack A, O'Garra A. Type I interferons in infectious disease. *Nat Rev Immunol*. 2015;15:87-103.
9. Tamura Y, Morikawa M, Tanabe R, Miyazono K, Koinuma D. Anti-pyroptotic function of TGF-β is suppressed by a synthetic dsRNA analogue in triple negative breast cancer cells. *Mol Oncol*. 2021;15:1289-1307.
10. Hobeika AC, Subramaniam PS, Johnson HM. IFNα induces the expression of the cyclin-dependent kinase inhibitor p21 in human prostate cancer cells. *Oncogene*. 1997;14:1165-1170.
11. Musella M, Manic G, De Maria R, Vitale I, Sistigu A. Type-I-interferons in infection and cancer: unanticipated dynamics with therapeutic implications. *Oncoimmunology*. 2017;6:e1314424.
12. Honda K, Takaoka A, Taniguchi T. Type I interferon gene induction by the interferon regulatory factor family of transcription factors. *Immunity*. 2006;25:349-360.
13. Escalante CR, Nistal-Villán E, Shen L, García-Sastre A, Aggarwal AK. Structure of IRF-3 bound to the PRDIII-I regulatory element of the human interferon-β enhancer. *Mol Cell*. 2007;26:703-716.
14. Perng YC, Lenschow DJ. ISG15 in antiviral immunity and beyond. *Nat Rev Microbiol*. 2018;16:423-439.
15. Xu P, Bailey-Bucktrout S, Xi Y, et al. Innate antiviral host defense attenuates TGF-β function through IRF3-mediated suppression of Smad signaling. *Mol Cell*. 2014;56:723-737.
16. Schild-Hay LJ, Leil TA, Divi RL, Olivero OA, Weston A, Poirier MC. Tamoxifen induces expression of immune response-related genes in cultured normal human mammary epithelial cells. *Cancer Res*. 2009;69:1150-1155.
17. Tudoran O, Virtic O, Balacescu L, et al. Baseline blood immunological profiling differentiates between Her2-breast cancer molecular subtypes: implications for immunomediated mechanisms of treatment response. *Onco Targets Ther*. 2015;8:3415-3423.
18. Alsaleem M, Toss MS, Joseph C, et al. The molecular mechanisms underlying reduced E-cadherin expression in invasive ductal carcinoma of the breast: high throughput analysis of large cohorts. *Mod Pathol*. 2019;32:967-976.
19. Hu F, Zhang Y, Li M, Bai Y, Zhang X. Expression and role of HEPIS in breast cancer. *Oncol Lett*. 2019;18:6648-6656.
20. Granqvist V, Holmgren C, Larsson C. Induction of interferon-beta and interferon signaling by TRAIL and Smac mimetics via caspase-8 in breast cancer cells. *PLoS One*. 2021;16:e0248175.
21. Harada M, Morikawa M, Ozawa T, et al. Palbociclib enhances activin-SMAD-induced cytostasis in estrogen receptor-positive breast cancer. *Cancer Sci*. 2019;110:209-220.
22. Isogaya K, Koinuma D, Tsutsumi S, et al. A Smad3 and TTF-1/NKX2-1 complex regulates Smad4-independent gene expression. *Cell Res*. 2014;24:994-1008.
23. Katsuno Y, Meyer DS, Zhang Z, et al. Chronic TGF-β exposure drives stabilized EMT, tumor stemness, and cancer drug resistance with vulnerability to bitopic mTOR inhibition. *Sci Signal*. 2019;12:eaau8544.
24. Katsuno Y, Hanyu A, Kanda H, et al. Bone morphogenetic protein signaling enhances invasion and bone metastasis of breast cancer cells through Smad pathway. *Oncogene*. 2008;27:6322-6333.
25. Borden EC. Interferons α and β in cancer: therapeutic opportunities from new insights. *Nat Rev Drug Discov*. 2019;18:219-234.
26. Doherty MR, Cheon H, Junk DJ, et al. Interferon-β represses cancer stem cell properties in triple-negative breast cancer. *Proc Natl Acad Sci USA*. 2017;114:13792-13797.
27. Doherty MR, Parvani JG, Tamagno I, et al. The opposing effects of interferon-β and oncostatin-M as regulators of cancer stem cell plasticity in triple-negative breast cancer. *Breast Cancer Res*. 2019;21:54.
28. Batlle E, Massagué J. Transforming growth factor-β signaling in immunity and cancer. *Immunity*. 2019;50:924-940.
29. Ulloa L, Doody J, Massagué J. Inhibition of transforming growth factor-β/SMAD signalling by the interferon-γ/STAT pathway. *Nature*. 1999;397:710-713.
30. Gorelik L, Constant S, Flavell RA. Mechanism of transforming growth factor β-induced inhibition of T helper type 1 differentiation. *J Exp Med*. 2002;195:1499-1505.
31. Lin JT, Martin SL, Xia L, Gorham JD. TGF-β1 uses distinct mechanisms to inhibit IFN-γ expression in CD4+ T cells at priming and at recall: differential involvement of Stat4 and T-bet. *J Immunol*. 2005;174:5950-5958.
32. Qin BY, Liu C, Lam SS, et al. Crystal structure of IRF-3 reveals mechanism of autoinhibition and virus-induced phosphoactivation. *Nat Struct Biol*. 2003;10:913-921.
33. Takahasi K, Suzuki NN, Horiuchi M, et al. X-ray crystal structure of IRF-3 and its functional implications. *Nat Struct Biol*. 2003;10:922-927.
34. Mori M, Yoneyama M, Ito T, Takahashi K, Inagaki F, Fujita T. Identification of Ser-386 of interferon regulatory factor 3 as critical target for inducible phosphorylation that determines activation. *J Biol Chem*. 2004;279:9698-9702.

SUPPORTING INFORMATION

Additional supporting information may be found in the online version of the article at the publisher's website.

How to cite this article: Tamura Y, Tsutsumi S, Miyazono K, Koinuma D. PolyI:C attenuates transforming growth factor-β signaling to induce cytostasis of surrounding cells by secreted factors in triple-negative breast cancer. *Cancer Sci*. 2022;113:940–949. doi:10.1111/cas.15241